Invited Paper

Task-based assessment of deformable mirrors

Thomas Farrell, Elizabeth Daly, Eugenie Dalimier and Chris Dainty

Applied Optics Group, Department of Experimental Physics,
National University of Ireland, Galway, Ireland.

ABSTRACT

A performance comparison is made using a number of commercially available Deformable Mirrors(DM) in fitting both ocular and atmospheric wavefronts. Least squares phase fitting simulations are performed for five mirrors using experimentally obtained mirror influence functions. The DMs used cover a range of DM technologies with varying size and cost. The phase fitting performance of these mirrors is found to be a function of influence function shape, actuator density and available mirror stroke.

Keywords: Deformable mirror, MEMS, adaptive optics,

1. INTRODUCTION

Deformable mirror technology has evolved to provide phase correction with ever increasing stroke magnitudes and actuator numbers. Adaptive Optics(AO) has been the main driving force behind DM use where they were first used in astronomical and satellite imaging systems. Other uses of adaptive mirrors include high-power laser beam shaping which has been achieved using micromachined membrane mirrors[1] and bimorph mirrors.[2] Adaptive optics for imaging the human eye was first achieved using piezoelectric DM technology. Since then other devices such as bimorph,[3] membrane[4] and liquid crystal spatial light modulators[5] have been used.

The devices under investigation here are only tested for their spatial shaping abilities. The dynamic nature of both atmospheric and ocular AO is ignored as is any actuator hysteresis present. Such effects could limit a particular mirrors usability particularly in astronomy where higher temporal frequency operation is important. Also it is assumed that the influence functions for each mirror add linearly. This study is a continuation of a previous one,[6] in which only three DMs were assessed for fitting of ocular wavefronts. The results presented should be viewed as guideline for performance expectations. Practical experimentation may lead to different results and possible unseen advantages/disadvantages such as ease of use, fragility etc.

2. DEFORMABLE MIRRORS

In this study the wavefront fitting performance of five DMs is calculated for both atmospheric and ocular abberations. This follows on from a previous characterisation study.[7] The five mirrors are as follows,

- A 19-channel piezoelectric mirror from Flexible Optical BV (OKO19).
- A 37-channel bulk micro-machined membrane mirror from the same manufacturer (OKO37)
- A 35-channel electrostrictive bimorph DM produced by AOptix (AOptix35)
- A 52 channel magnetic membrane mirror from Imagine Eyes (MIRAO52)
- A 140 channel MEMS device which is manufactured by Boston Micromachines (BMC140)

Further author information: (Send correspondence to C.D.)
E.D.: E-mail: elizabeth.daly@nuigalway.ie, Telephone: +353 (0)91 492985
Eu.D.: E-mail: eugenie.dalimier@nuigalway.ie, Telephone: +353 (0)91 495191
C.D.: E-mail: c.dainty@nuigalway.ie, Telephone: +353 (0)91 512374
T.F.: E-mail: thomas.d.farrell@gmail.com, Telephone: +353 (0)91 495350

MEMS Adaptive Optics, edited by Scot S. Olivier, Thomas G. Bifano, Joel A. Kubby,
Proc. of SPIE Vol. 6467, 64670F, (2007) · 0277-786X/07/$18 · doi: 10.1117/12.707600

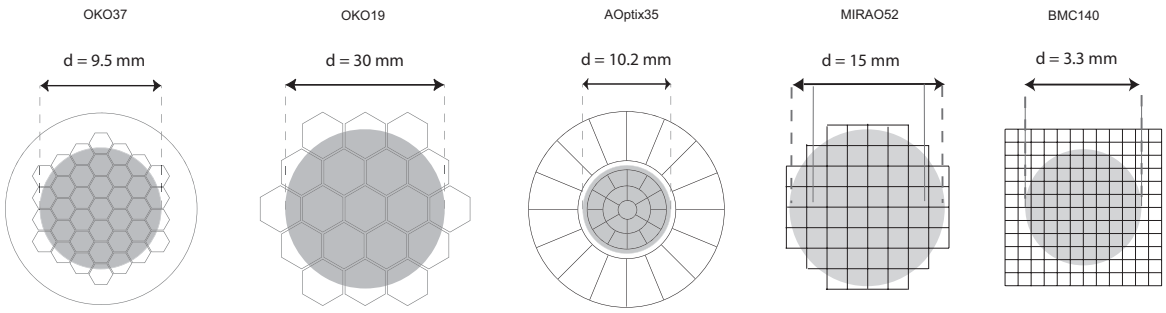

Figure 1. Schematic for each mirror showing the orientation and shape of actuators as well as the pupil sizes used for testing. Points outside the shaded areas were not used for evaluating wavefront fitting

Mirror	Technology	Diameter (mm)	Actuators	Stroke (μm)	Approx. price (US$)
OKO37	Electrostatic	15	37	3.5	5000
OKO19	Piezoelectric	30	19	3, 7-9	8000
AOptix35	Electrorestrictive	10.2	35	16	30000
MIRAO52	Magnetic	15	52	50	26000
BMC140	Electrostatic	3.3 x 3.3	140	3.5	35000

Table 1. Details of DMs tested. The diameter is the full diameter of the mirror but for some devices only a fraction of this diameter is used.

The influence functions for each of these mirrors were measured using a FISBA Twyman Green Interferometer.The influence function matrix $\mathbf{M}$, relates actuator signals to a resulting phase map, ϕ and are all thats required experimentally to evaluate a mirrors phase fitting performance.

$$\phi = \mathbf{M}v. \tag{1}$$

To minimise some wavefront, ϕ_m the control signals to be sent to the mirror are given as

$$v = \mathbf{M}^{-1}\phi_m \tag{2}$$

As the $\mathbf{M}$ is generally rectangular and thus non-invertible, it is decomposed into the invertible Singular Value Decomposition form.

$$\mathbf{M} = \mathbf{U}\mathbf{W}\mathbf{V}^T. \tag{3}$$

Using the pseudo inverse of this new form of $\mathbf{M}$ the control commands can then be calculated as

$$v = \mathbf{V}\mathbf{W}^{-1}\mathbf{U}^T\phi. \tag{4}$$

These control signals are then clipped to account for the limited range of motion of the mirror's actuators.

The size, shape and stroke of a single actuator influence function is a good indication of its fitting abilities, ie. wide influence functions with small peak to valley (PV) deformations will lead to poor fitting and stroke-limited corrections. Table 1 shows the main properties of these five mirrors whilst Fig. 1 gives a schematic of the actuator arrangements and pupil sizes used for each mirror.

3. SIMULATION RESULTS

3.1. Fitting atmospherically aberrated wavefronts

The earth's atmosphere has an aberrating effect on any light that is passed through it the effects of which are well described statistically by Komolgorov theory[8] In this study we are just concerned with light propagated

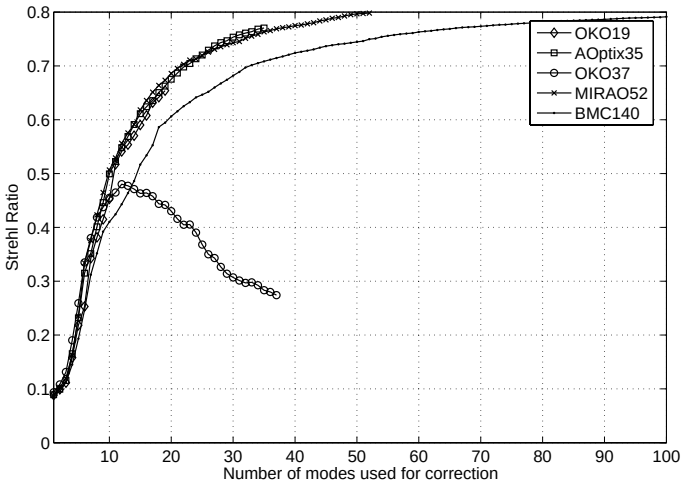

Figure 2. Strehl ratio after fitting the five mirrors to a sample of 100 atmospheric wavefronts with $(D/r_0) = 6$

vertically through turbulence as is the case in astronomy. The Fried parameter, r_0, is a common metric used to describe the strength of turbulence over a particular pupil area. It is related to the phase variance σ_ϕ^2, by

$$\sigma_\phi^2 = 1.03(D/r_0)^{5/3} \tag{5}$$

where D is the diameter of the telescope pupil. Larger values of D/r_0 require higher actuator densities and stroke capabilities from a DM.

For this study, large numbers of atmospheric wavefronts were generated according to the Komolgorov theory with varying degrees of strength (D/r_0= 6,9,12); these values would be appropriate for an 8m telescope correcting in the K band ($2.2\mu m$) with r_0 equal to $0.67 - 1.33m$. The piston and tip/tilt components of these wavefronts were removed to replicate the operation of a real AO system and to avoid early DM saturation. For each sample of turbulence the control commands are calculated for a particular mirror using Eq. 4. The residual root mean square wavefront error (μm) is then estimated as

$$\phi_{res} = \phi_m - \mathbf{M}v \tag{6}$$

Imaging performance can be characterised using the residual rms error but here the Strehl Ratio (SR) will be used as it is the more common astronomical image quality metric. SR can be calculated using the Marechal approximation as

$$\mathbf{SR} = e^{-(\phi_{res})^2} \tag{7}$$

When performing a correction only a certain number of mirror modes should be included to avoid saturation from 'noisy' actuators. When an actuator has a very small effect on phase (ie. edge actuators, malfunctioning actuators) it will quickly saturate when asked to perform even moderate phase fittings which leads to fitting errors. These low gain modes should be excluded by zeroing the appropriate singular value. An analysis of optimum mode inclusion is given in figures 2, 3 and 4.

The simulated turbulence with $(D/r_0) = 6$ is quite weak and well within the limits of most of the mirrors with the exception of the OKO37. It has a large number of low gain mirror modes which saturate quickly and limit correction performance. Including more than 12-15 modes for correction leads to saturation, in effect reducing the DM's already limited number of actuators. The OKO19 performs much better due to its higher available

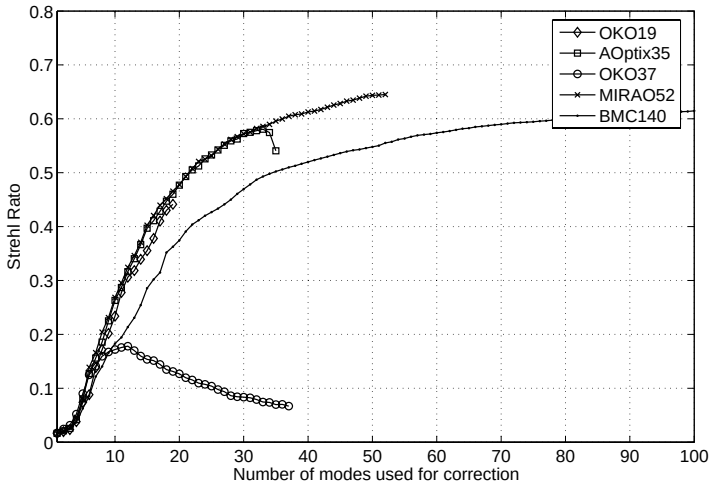

Figure 3. Strehl ratio after fitting the five mirrors to a sample of 100 atmospheric wavefronts with $(D/r_0) = 9$

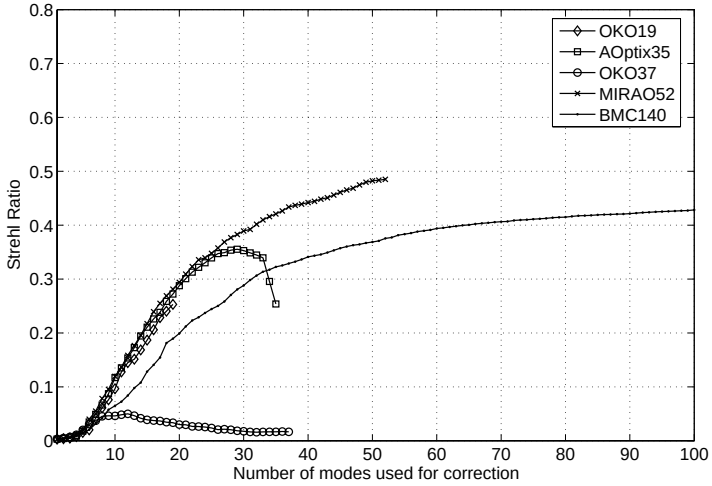

Figure 4. Strehl ratio after fitting the five mirrors to a sample of 100 atmospheric wavefronts with $(D/r_0) = 12$

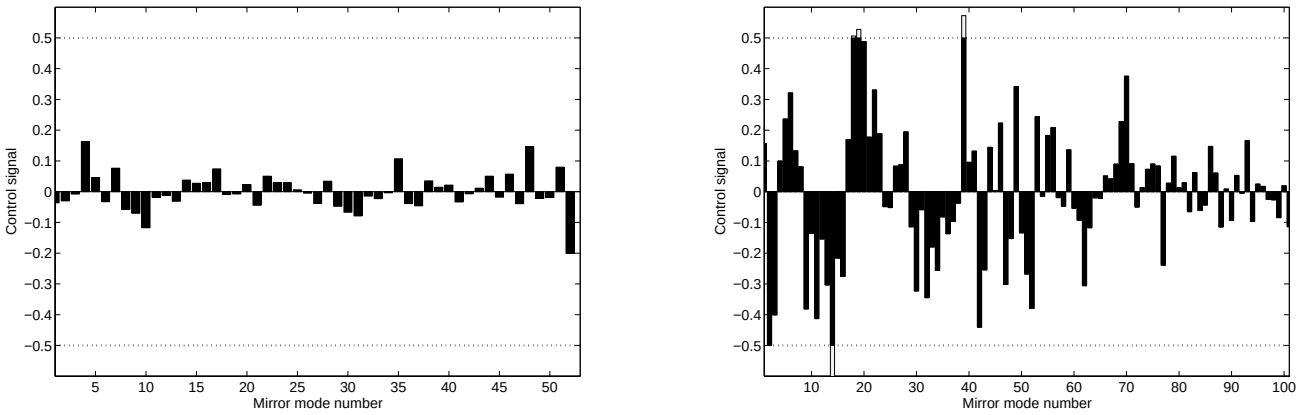

Figure 5. Snapshot of actuator commands for the MIRAO52 (left) and the BMC140 (right). Clipped commands can be seen with white bars. Turbulence strength $(D/r_0) = 12$

stroke and is quite a capable mirror for correction of lower order abberations. At higher turbulence strengths its limited number of actuators impacts on its wavefront fitting ability.

The AOptix35 performs well throughout, showing slight saturation as turbulence strength is increased. At these stronger levels, the MIRAO has the best correcting performance with Strehl ratios near 0.5 achievable for $(D/r_0) = 12$. The BMC140 does not match this performance despite having far more actuators available. This is due to its limited stroke which, when compared with the MIRAO52, causes actuator clipping (Fig. 5).

3.2. Fitting ocular wavefronts

The abberations associated with the human eye do not share the same statistics as that of the atmosphere. As yet there is still no well-defined statistical theory to describe these aberrations. However there is available experimental data for large samples of healthy, well corrected (astigmatism and defocus minimised) eyes.[9,10] Using 100 samples of such eyes, the previous simulation was repeated for all five mirrors and a plot of the residual root mean square error was made as a function of mirror modes included (Fig.6).

For these samples of eye abberations there was an initial average rms wavefront error of $0.69\mu m$, which is approximately the average wavefront error for the $D/r_0 = 9$ turbulence wavefronts. The rhs of the figure shows the correction obtained, expressed as rms wavefront aberration for the case of $D/r_0 = 9$. The level of correction is not as low as for typical eye wavefronts as in the atmospheric case, higher order modes are not corrected.

4. CONCLUSION

We have tested a wide range of DMs for their wavefront fitting ability for both atmospheric and ocular aberrations. It is assumed that the mirrors operate linearly and only their static spatial performance was taken into account. Despite the differences between the two sets of abberations we can observe similarities in the results. It is the mirrors with the higher stroke that tended to offer less fitting errors. The relatively low-order AOptix35, which is optimised for correcting ocular wavefronts, performs best at this task but tends to saturate when confronted with atmospheric wavefronts. The BMC140 is quite a capable mirror but is limited by its stroke, whilst the MIRAO with its huge $50\mu m$ stroke outperforms all when asked to correct for strong turbulence.

The importance of having a capable DM when operating AO cannot be underestimated. Some care should be taken when considering various DM designs. The performance of a particular DM is a function of

- the individual actuator stroke and overall mirror stroke. This should be matched to the job at hand

- the size and shape of actuator influence functions. Wide influence functions reduce the spatial correcting abilities of a mirror

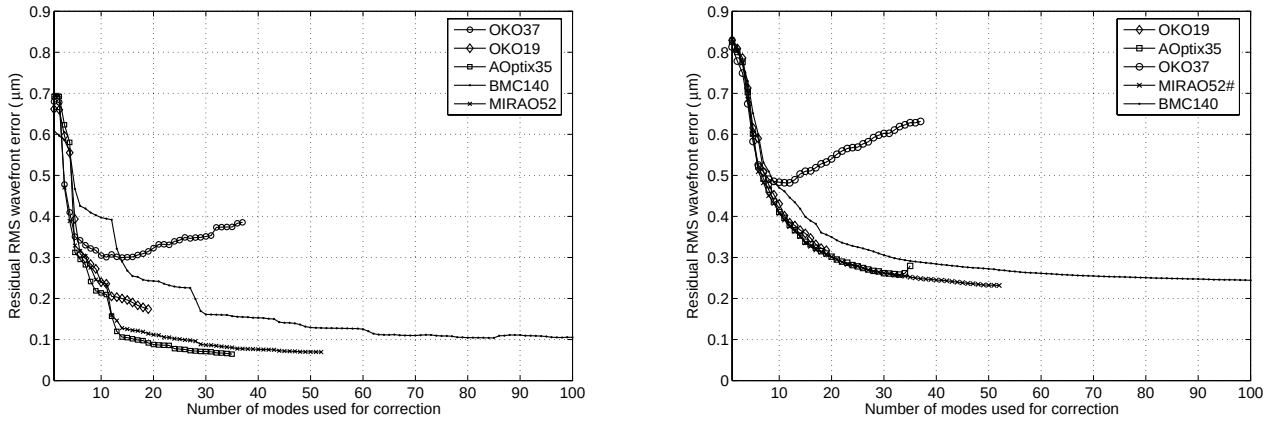

Figure 6. Residual rms wavefront error for five mirrors using the 100 samples of ocular wavefronts(left) Residual rms wavefront error for five mirrors using the 100 samples of atmospheric wavefronts (right)Turbulence stretch $(D/r_0) = 9$

- the number and arrangement of actuators.

Finally, some consideration must also be given to the cost of a device weighted against its performance requirements and also to the diameter of mirror surface. Small MEMS devices may not be suited to astronomical due to the large demagnification involved and likewise, ocular AO benefits from mirrors having comparable diameters to that of a human eye.

ACKNOWLEDGMENTS

We thank Larry Thibos and Gordon Kennedy for their previous contributions on which part of this study is derived.

This research is funded by Science Foundation Ireland under Grant No. SFI/01/PI.2/B039C, by a European Union EU Research Training Network, contract number HPRN-CT-2002-00301 "SHARP-EYE". and The Irish Research Council for Science Engineering and Technology under their postgraduate scholar scheme.

REFERENCES

1. E. Zeek, K. Maginnis, S. Backus, U. Russek, M. Murnane, G. Mourou, H. Kapteyn, and G. Vdovin, "Active trasverse mode control and optimisation of an all-solid-state laser using an intracavity adaptive-optic mirror," *Opt. Lett.* **24**, pp. 493–495, 1999.
2. T. Y. Cherezova, L. N. Kaptsov, and A. V. Kudryashov, "Cw industrial rod yag:nd3+ laser with an intra-cavity active bimorph mirror," *Appl. Opt.* **35**, pp. 2554–2561, 1996.
3. M. Glanc, E. Gendron, F. Lacombe, D. Lafaille, J.-F. L. Gargasson, and P. Léna, "Towards wide-field retinal imaging with adaptive optics," *Opt. Comm.* **230**, pp. 225–238, 2004.
4. E. J. Fernández, I. Iglesias, and P. Artal, "Closed-loop adaptive optics in the human eye," *Opt. Lett.* **26**, pp. 746–748, 2001.
5. F. Vargas-Martín, P. M. Prieto, and P. Artal, "Correction of the aberrations in the human eye with a liquid-crystal spatial light modulator: limits to performance," *J. Opt. Soc. Am. A* **15**, pp. 2552–2562, 1998.
6. E. Dalimier and C. Dainty, "Comparative analysis of deformable mirrors for ocular adaptive optics," *Opt. Exp.* **13**, pp. 4275–4285, 2005.
7. E. Daly, E. Dalimier, and C. Dainty, "Requirements for MEMS mirrors for adaptive optics in the eye," in *MEMS/MOEMS Components and Their Applications III*, S. S. Olivier, S. A. Tadigadapa, and A. K. Henning, eds., pp. 58–65, Jan. 2006.

8. D. L. Fried, "Optical resolution through a randomly inhomogeneous medium for very long and very short exposures," *J. Opt. Soc. Am. A.* **56**, pp. 1372–, 1966.
9. L. Thibos, R. A. Applegate, J. T. Schwiegerling, and R. Webb, "Standards for reporting optical aberrations of eyes," *J. Refract. Surg.* **18**, pp. 652–660, 2000.
10. L. Thibos, A. Bradley, and X. Hong, "A statistical model of the aberration structure of normal, well-corrected eyes," *Ophthal. Physiol. Opt.* **22**, pp. 427–433, 2002.